

Supporting Information for

Subseasonal prediction of extreme winter weather in California in a hybrid dynamical-statistical framework.

Kristen Guirguis¹, Alexander Gershunov¹, Benjamin J. Hatchett², Michael J. DeFlorio¹, Aneesh C. Subramanian³, Rachel Clemesha¹, Luca Delle Monache¹, and F. Martin Ralph¹

¹*Scripps Institution of Oceanography, University of California San Diego, La Jolla, California*

²*Desert Research Institute, Reno, NV*

³*University of Colorado Boulder, Boulder, Colorado*

Contents of this file

Text S1

Figures S1, S2, S3, S4, S5, S6, S7, S8, S9, S10

Introduction

This supporting information includes additional text about the varying model complexity of the statistical model (Text S1). Figure S1 shows the amount of joint variance explained by the NP4 modes in a region over the North Pacific Ocean and along the West Coast. Figure S2 shows the weather regimes of GGR'22 defined using the joint NP4 phase combinations. Figure S3 shows impacts associated with each weather regime. Figure S4 shows the three California regions used for the analysis of heat waves and cold extremes. Figure S5 shows the results of sensitivity tests to optimize the consensus threshold criteria. Figure S6 shows the varying complexity of the statistical model at different lead times for 21 years of hindcast data. Figure S7 shows the distribution of probabilistic forecasts along with the three forecast category bins and sample sizes. Figure S8 shows the validated NP4 mode phase forecasts for WY2022 using the ensemble mean. Figure S9 highlights the effects of the persistent positive phase of the Offshore-CA mode during January-February 2022. Figure S10 shows the hindcast skill assessment for cold extremes.

Text S1

Expanded Methods: The Varying Complexity of the Statistical Model

The statistical model (Equation 1) uses up to four predictors, but as shown in Figure 2 (steps 3-4), all four modes are not always available due to dynamical model uncertainty. Therefore, the complexity of the statistical model, defined as the number of variables used as predictors in Equation 1, varies from forecast to forecast. The full complexity model (N=4) is employed when the BP, AP, CP, and OC modes are all predicted with high confidence by the ECMWF model. However, the likelihood of reaching this level of confidence decreases with lead time. Figure S6 shows the number of modes (N) that were predicted with confidence (>70% ensemble agreement) for the 21 years of hindcasts. At short leads, most forecasts have reliable information about all four NP4 modes indicating a high level of model confidence about synoptic-scale atmospheric circulation. At longer lead times, this becomes less likely such that by day 14

this only occurs 10% of the time, meaning that the ECMWF model is uncertain about important circulation anomaly features over the domain of interest. In week 1, the ECMWF model generally provides information about 3-4 modes. In week 2, this reduces to 2-4 modes. By weeks 3-4, most forecasts are based on only 1-2 modes provided by the dynamical model. Also, at longer lead times, we see that the ECMWF model is increasingly uncertain about all modes ($N=0$). In these cases, when zero modes are forecast with confidence by the ECMWF model, our approach is to not issue a forecast with the hybrid model.

Supporting Figures

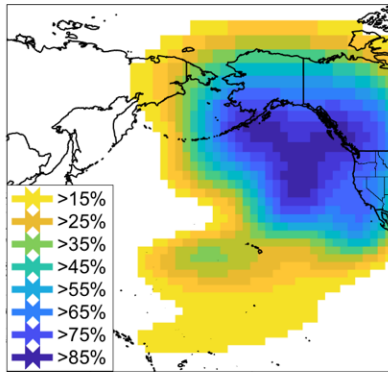


Figure S1. The percent of local Z500 variance explained by the NP4 modes using multiple linear regression (from Guirguis et al. 2022).

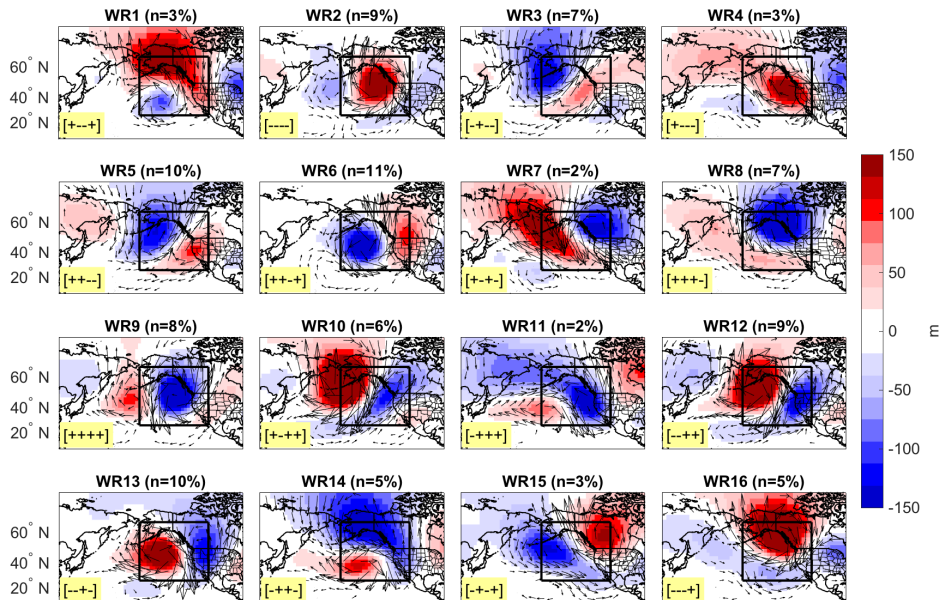


Figure S2. These sixteen weather regimes, shown as composites of 500 mb geopotential height anomalies, were defined in GGR'22 based on the joint phase combinations of the NP4 modes. As the NP4 modes fluctuate over the course of a season, they come in and out of phase with each other, and these different phase combinations produce the weather patterns shown above. The

NP4 phase combination for each weather regime is shown as highlighted text in the lower left corner, where the +/- indicates the phase of each NP4 mode in the following order: [BP, AP, CP, OC]. The sample size for each composite (n) is given in the title as a percentage of total days in the record spanning 1948-2017. From GGR'22.

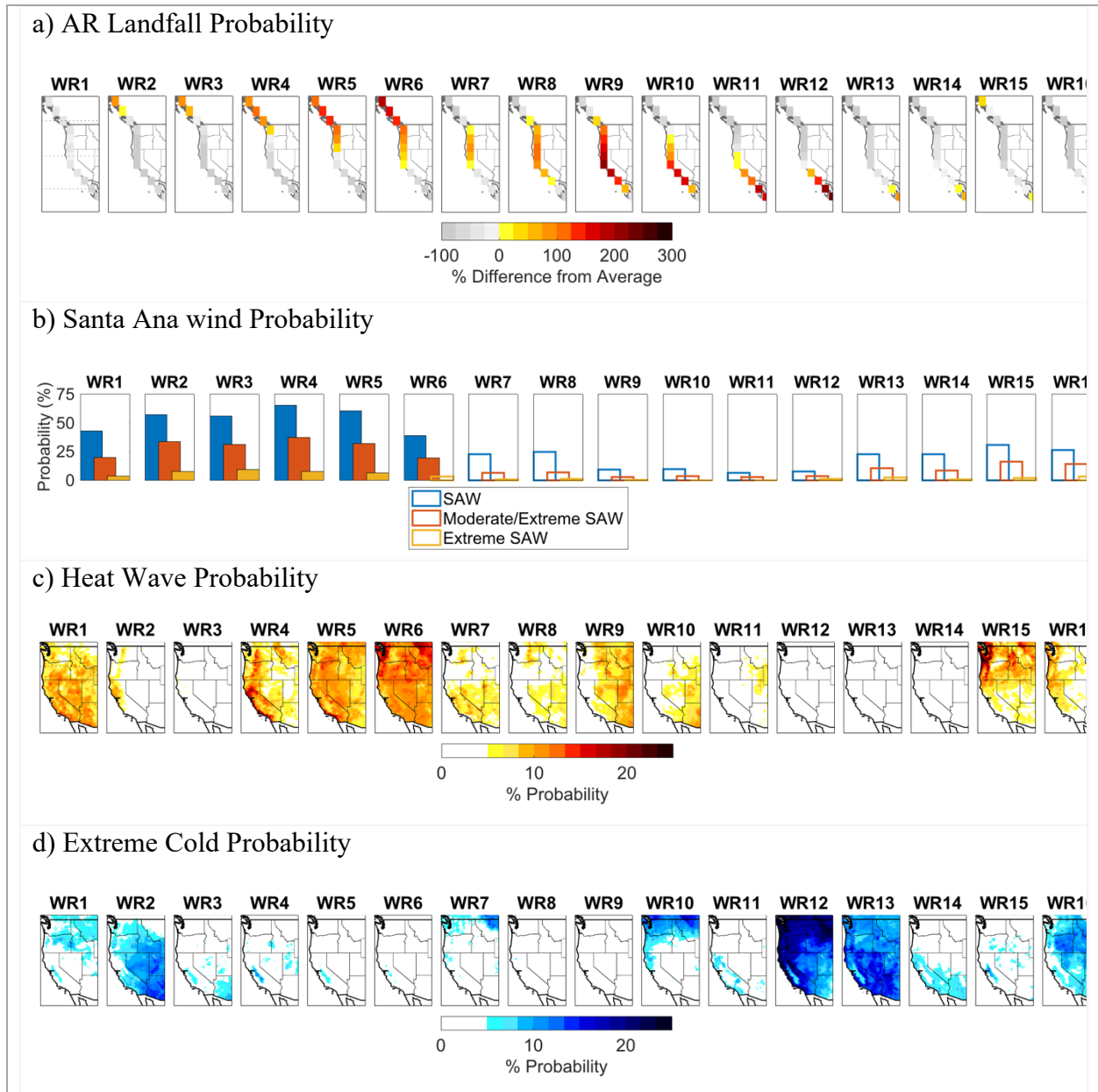


Figure S3. Impacts associated with each of the sixteen weather regimes shown in Figure S2 (from GGR'22) showing the historical probabilities of AR landfalls (b), extreme heat (c), and extreme cold (d) conditional on the observed atmospheric weather regime. From GGR'22.

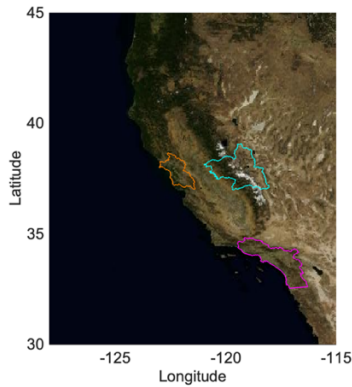


Figure S4. Map showing the location of the Central Sierra Nevada Mountain region (blue) coastal Southern California (pink), and San Francisco Bay (orange) which are used in this study to validate the heat wave forecasts. The satellite data are from NASA’s Earth Observing System Data and Information System (EOSDIS). The regions are defined using shapefiles from the Department of Water Resources.

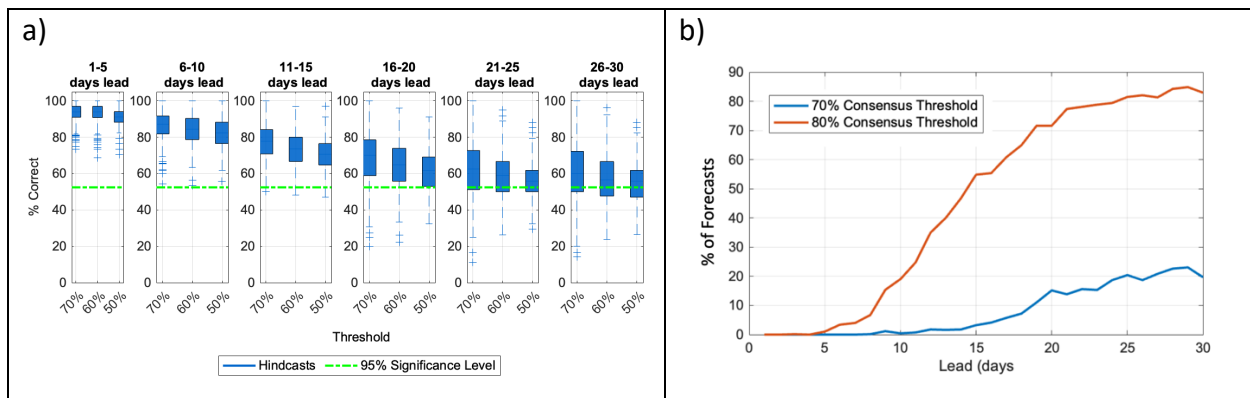


Figure S5. Sensitivity tests for optimizing the consensus threshold used in the statistical model. (a) shows the percent of correct NP4 mode phase forecasts using different thresholds: 70%, 60%, and 50% ensemble member agreement, noting higher skill using the 70% criteria. (b) shows the percent of forecasts in which 70% or 80% agreement is not met (i.e., the model ensemble members generally do not agree at the 80% level in weeks 3-4; by day 15 less than half of forecasts meet the 80% agreement criteria).

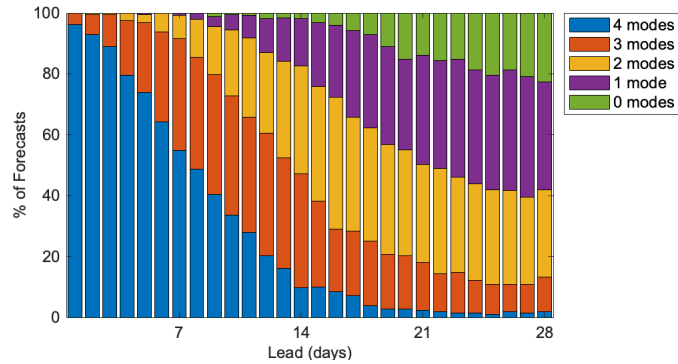


Figure S6. Showing the varying complexity of the statistical model by lead time. The y-axis gives the proportion of the hindcasts in the 22-year record, and the color scale indicates the number of modes (N) used as input into the statistical model (Equation 1).

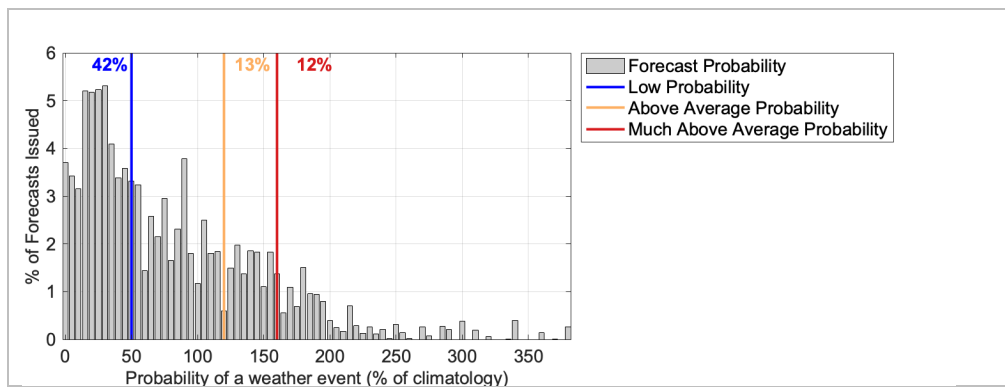


Figure S7. Frequency distribution of all 1-30-day probabilistic forecasts issued by the hybrid model including for temperature extremes, SAWs, and AR landfalls, along with the thresholds for the three forecast categories. The percentage of forecasts in each bin category (42%, 13%, 12%) is shown as text in the plot.

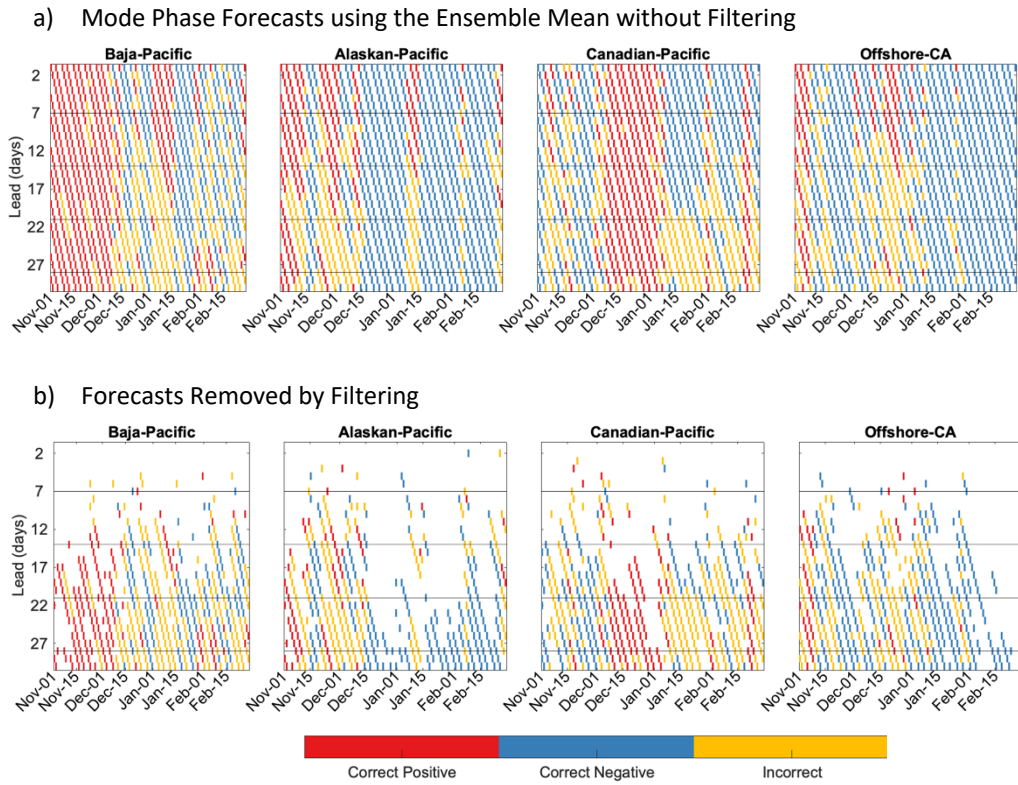


Figure S8. Shows the effectiveness of the consensus filtering approach, where panel (a) is the same as Figure 1b but for a reference forecast using the ensemble mean with no filtering and (b) shows the forecasts that would have been issued using the ensemble mean approach, but which were filtered out using the 70% consensus criteria (i.e., the difference between Figure S4a and Figure 1b).

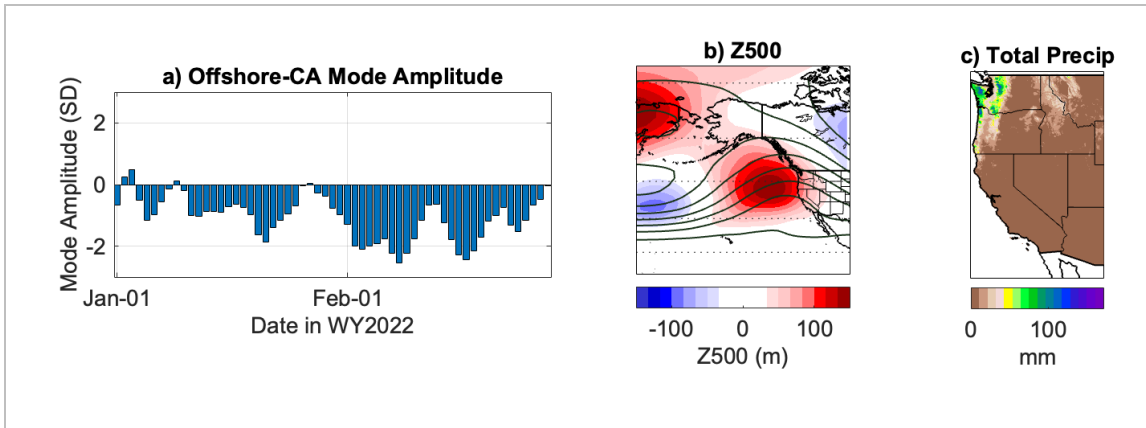


Figure S9. (a) Observed amplitude of the Offshore-CA mode during January-February 2022 to highlight the persistent negative phase. (b) Composite of observed Z500 anomalies over Jan1-Feb 28, 2022. (c) Total precipitation that fell during Jan1-Feb 28, 2022.

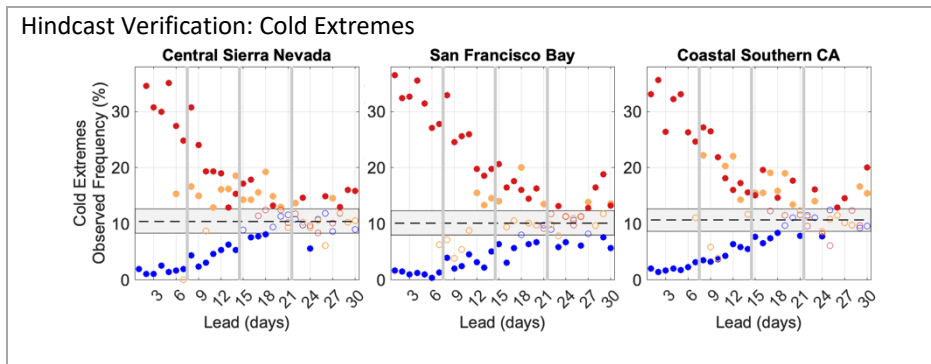


Figure S10. As in Figure 3b but for cold extremes.